

# A combination of drug screen and RNA landscape reveals targetable pathways in HIV-1 reactivation

Yang-Hui (Jimmy) Yeh<sup>1</sup>, Katharine Jenike<sup>2</sup>, Rachela Calvi<sup>3</sup>, Jennifer Chiarella<sup>3</sup>, Rebecca Hoh<sup>4</sup>, Steven G Deeks<sup>4</sup>, Ya-Chi Ho<sup>1</sup>

<sup>1</sup>Department of Microbial Pathogenesis, Yale University; <sup>2</sup>Department of Medicine, Johns Hopkins University; <sup>3</sup>Department of Neurology, Yale University;

<sup>4</sup>Department of Medicine, University of California, San Francisco



Yale SCHOOL OF MEDICINE



## BACKGROUND

**Background.** Despite effective antiretroviral therapy, HIV-1-infected cells continue to produce viral antigens and induce chronic immune exhaustion. We propose to identify HIV-1-suppressing agents which can inhibit HIV-1 reactivation and reduce HIV-1-induced immune activation.

**Approaches.** We developed a dual-reporter cell line model and screened a library of 1,430 FDA-approved small molecule compounds to identify HIV-1-suppressing agents. Second, we examined the effect of candidate HIV-1-suppressing agents on HIV-1 transcription and HIV-1-driven aberrant host gene transcription at the integration site. Third, we examined cellular transcriptional landscape of cells treated with candidate HIV-1-suppressing agents using three transcriptome analyses to find distinct pathways how these agents affect host cell environment. Fourth, to understand whether candidate HIV-1-suppressing agents can disrupt the proliferation dynamics of HIV-1-infected cells, we examined the frequency of HIV-1-infected cells from HIV-1-infected individuals upon ex vivo T cell activation with and without ex vivo treatment of candidate HIV-1-suppressing agents.

## METHOD AND RESULTS

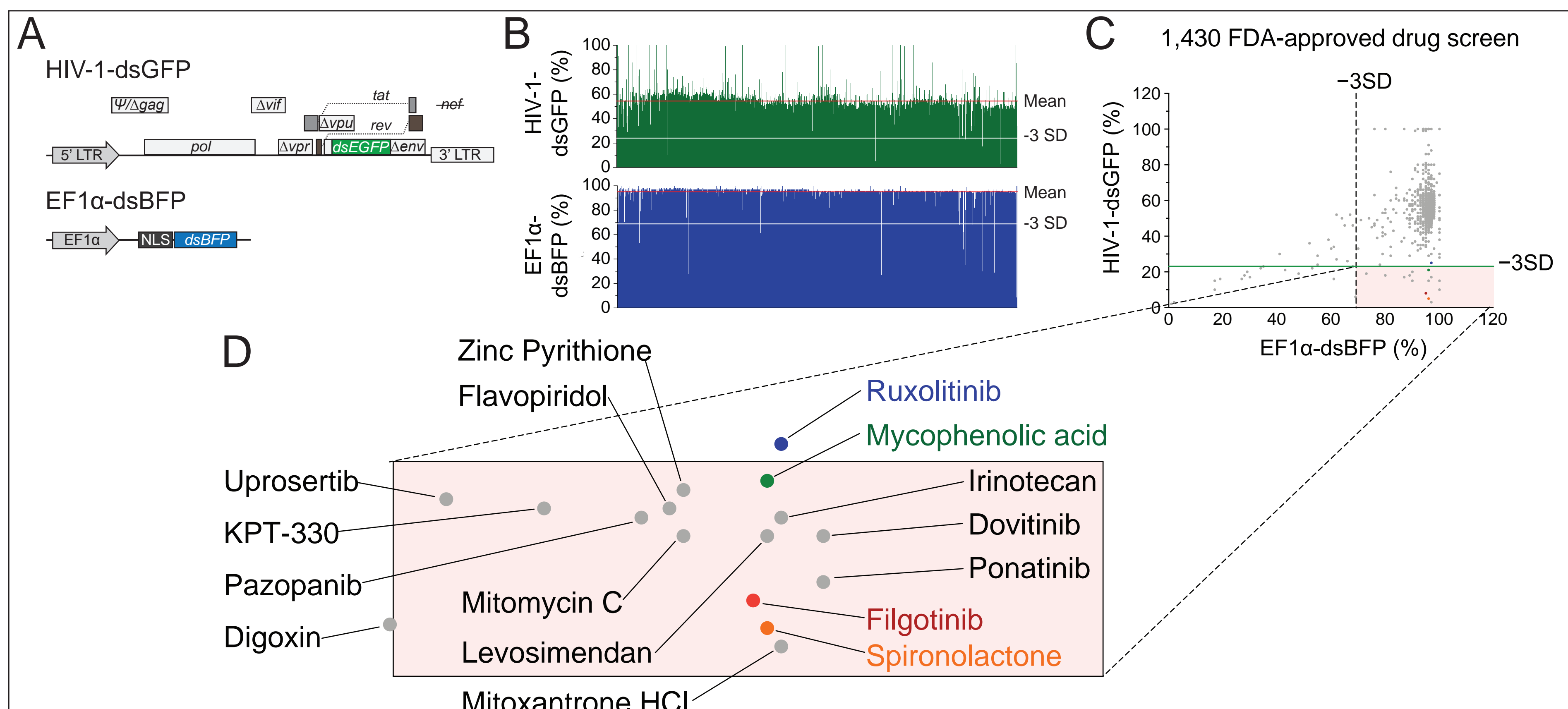


**Figure 1.** An FDA-approved small molecule compound library screen identified HIV-1-suppressing agents. (A) Scheme of the lentiviral reporter constructs. (B) A small molecule compound library of 1,430 FDA-approved drugs were screened in 96-well plates. (C, D) Screening of FDA-approved drug library identified 16 HIV-1-suppressing agents.

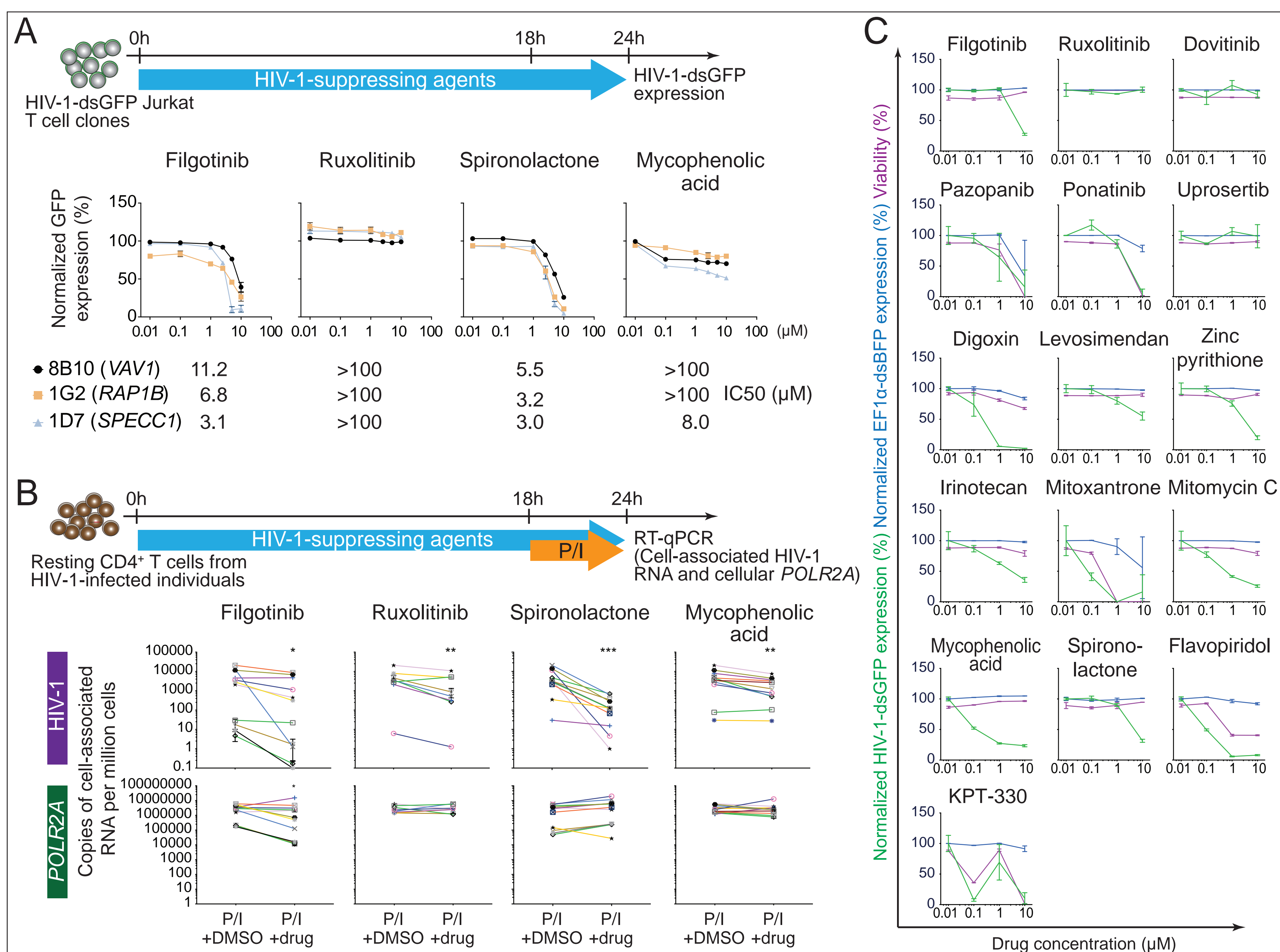


**Figure 2.** HIV-1-suppressing agents inhibit HIV-1 expression. (A) Dose response curves of candidate HIV-1-suppressing agents in three cell line models. HIV-1-dsGFP expression levels were normalized to the levels in DMSO-treated samples. Error bars represent standard errors from quadruplicates. (B) Cell-associated RNA levels of polyadenylated HIV-1 and a housekeeping gene *POLR2A* in CD4<sup>+</sup> T cells from virally suppressed HIV-1-infected individuals upon treatment with HIV-1-suppressing agents and PMA/ionomycin challenge in the presence of ART. (C) Dose response curves of HIV-dsGFP, EF1α-dsBFP, and viability in HIV-1-suppressing agents treatment. The expression levels were normalized to that of DMSO-treated controls. GFP, green fluorescent protein. BFP, blue fluorescent protein. NLS, nuclear localization signal. P/I, PMA/ionomycin. DMSO, dimethylsulfoxide. \*, p < 0.05; \*\*, p < 0.01; \*\*\*, p < 0.001 by two-tailed paired Student's t-test. Error bars represent standard errors from triplicates.

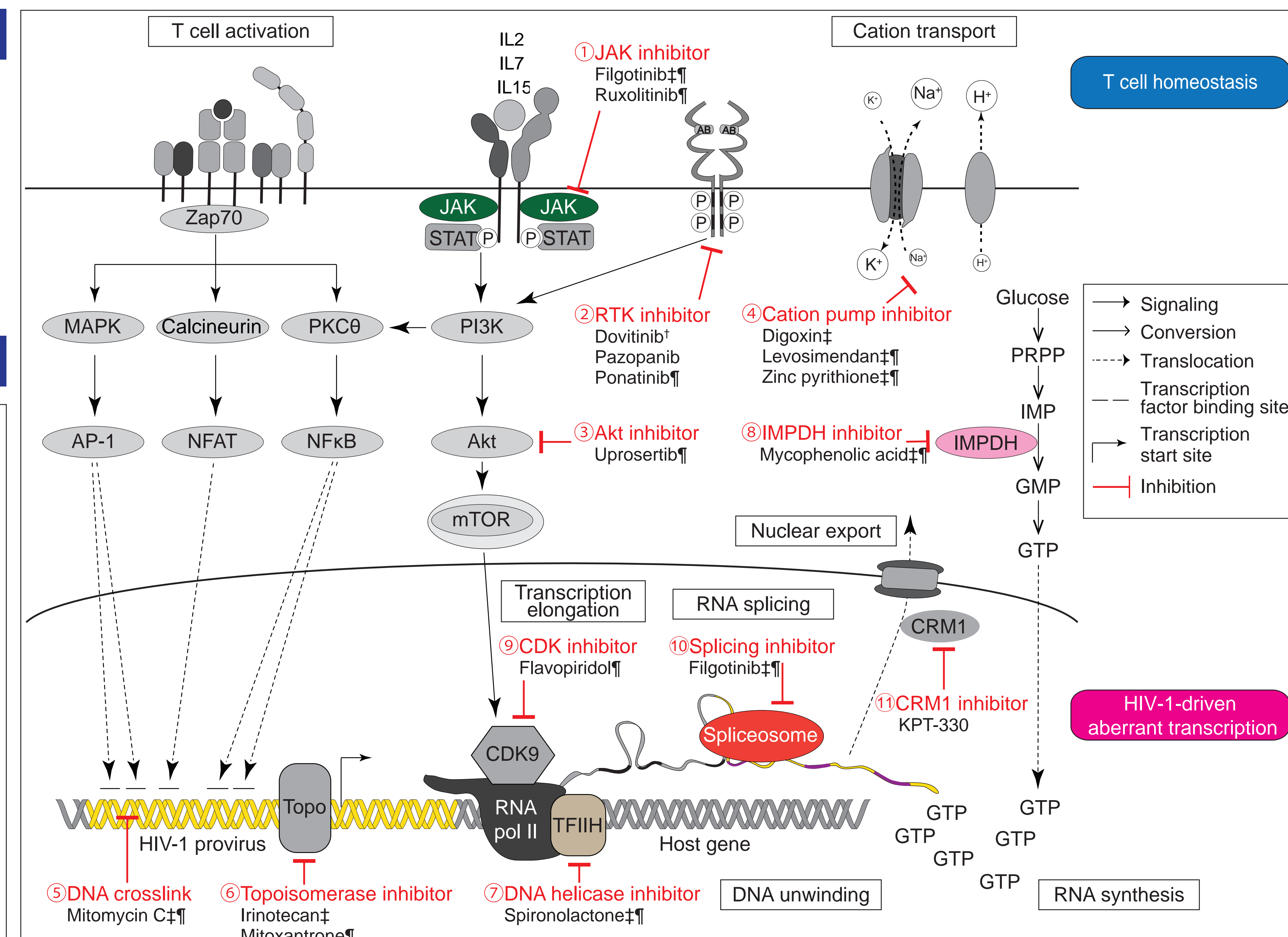


**Figure 3.** Therapeutic targets of HIV-1 reactivation. A high-throughput drug screen identified 11 cellular pathways critical for HIV-1 transcription after HIV-1 integration. †, preferential HIV-1 suppression in one additional cell line. ‡, HIV-1 suppression in two additional cell lines. ††, HIV-1 suppression in CD4<sup>+</sup> T cells from virally suppressed HIV-1-infected individuals.

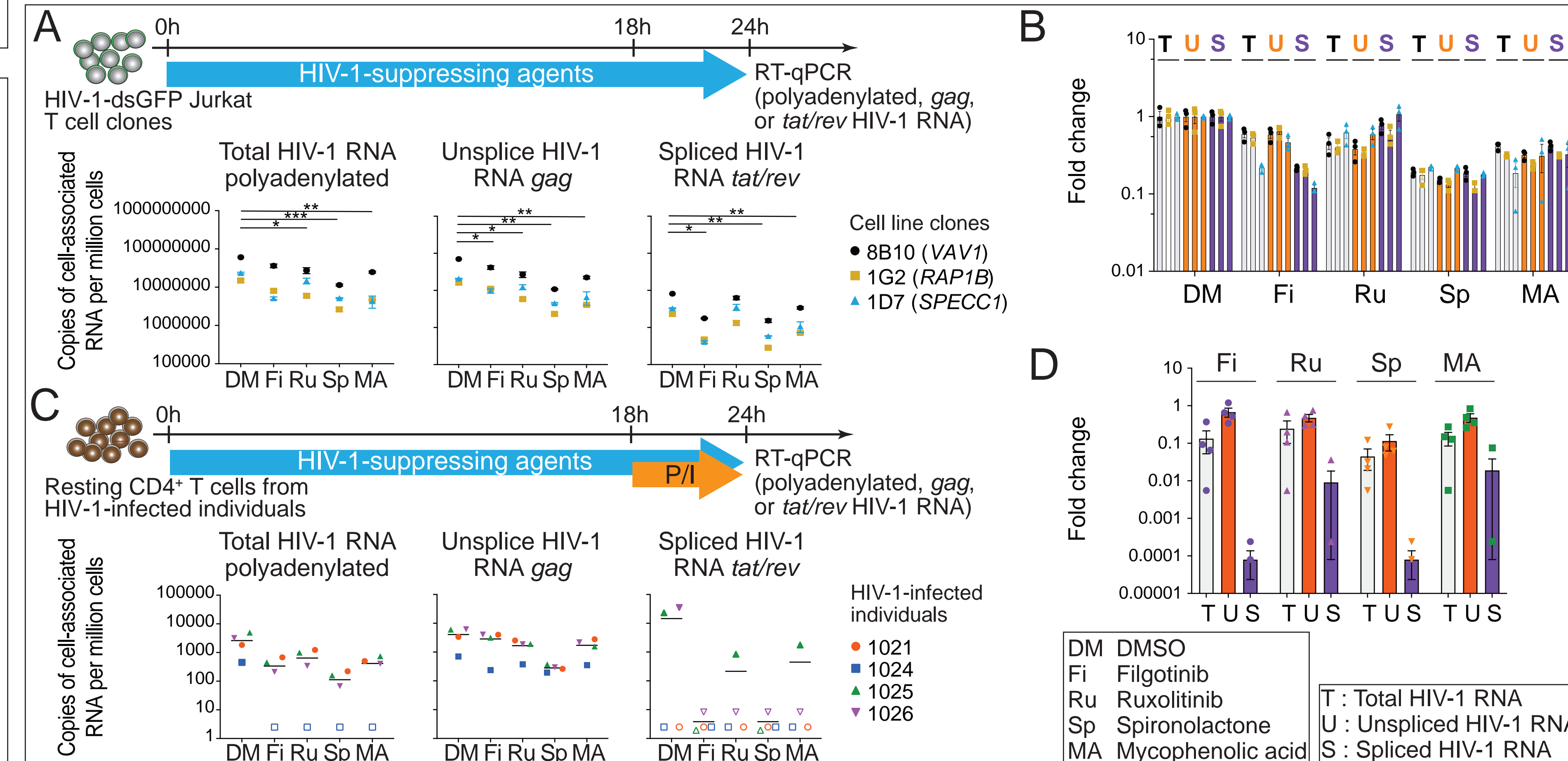


**Figure 4.** HIV-1-suppressing agents reduce different levels of spliced and unspliced HIV-1 RNA transcription. Cell-associated RNA levels (A, C) and fold inhibition (B, D) of total (polyadenylated), unspliced (*gag*), and spliced (*tat/rev*) HIV-1 RNA in three HIV-1-dsGFP-Jurkat clones (A, B) and CD4<sup>+</sup> T cells from virally suppressed, HIV-1-infected individuals (C, D) were measured by RT-qPCR. Error bars represent standard errors from quadruplicates.

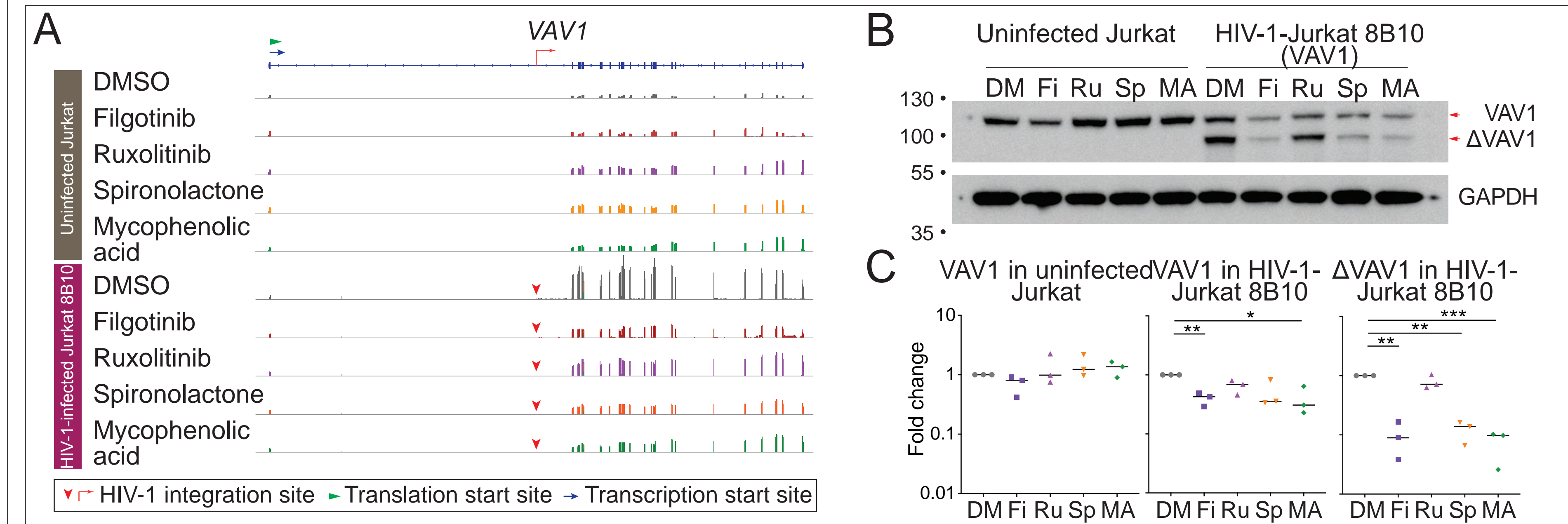


**Figure 5.** HIV-1-suppressing agents reduce HIV-1-driven aberrant host gene transcription at the integration site. (A) Normalized transcriptional landscape using first exon in the HIV-1-Jurkat clone 8B10. Red arrowhead, HIV-1 integration site mapped by inverse PCR. (B) Western blot of VAV1 protein expression in HIV-1-infected Jurkat clone 8B10 treated with HIV-1-suppressing agents. (C) Relative quantification of intact VAV1 and truncated VAV1 expression to DMSO treatment normalized to GAPDH in triplicates.

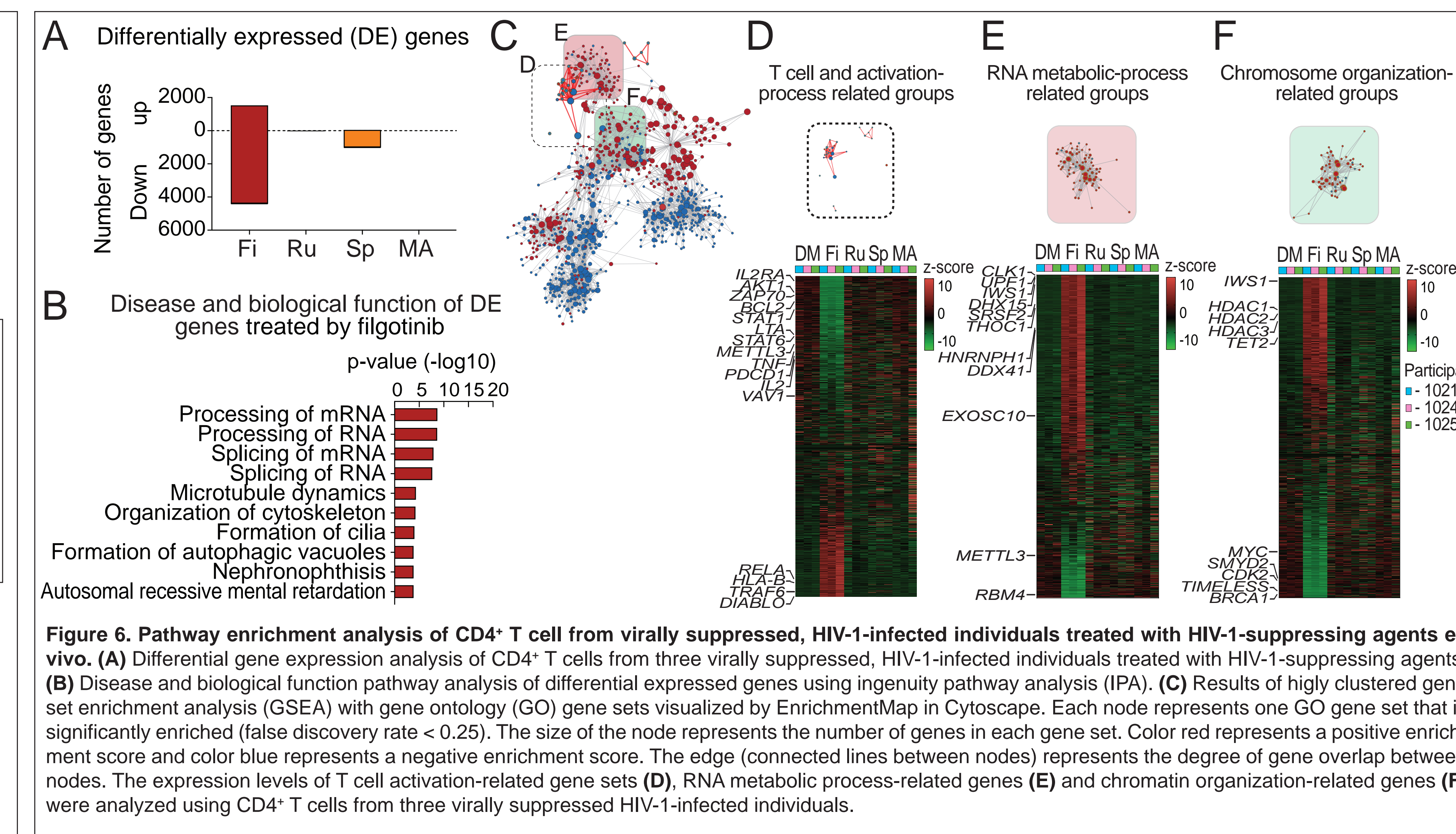


**Figure 6.** Pathway enrichment analysis of CD4<sup>+</sup> T cell from virally suppressed, HIV-1-infected individuals treated with HIV-1-suppressing agents ex vivo. (A) Differential gene expression analysis of CD4<sup>+</sup> T cells from three virally suppressed, HIV-1-infected individuals treated with HIV-1-suppressing agents. (B) Disease and biological function pathway analysis of differentially expressed genes using ingenuity pathway analysis (IPA). (C-E) Results of highly clustered gene set enrichment analysis (GSEA) with gene ontology (GO) gene sets visualized by EnrichmentMap in Cytoscape. Each node represents one GO gene set that is significantly enriched (false discovery rate < 0.25). The size of the node represents the number of genes in each gene set. Color red represents a positive enrichment score and color blue represents a negative enrichment score. The edge (connected lines between nodes) represents the degree of gene overlap between nodes. The expression levels of T cell activation-related gene sets (D), RNA metabolic process-related genes (E) and chromatin organization-related genes (F) were analyzed using CD4<sup>+</sup> T cells from three virally suppressed HIV-1-infected individuals.

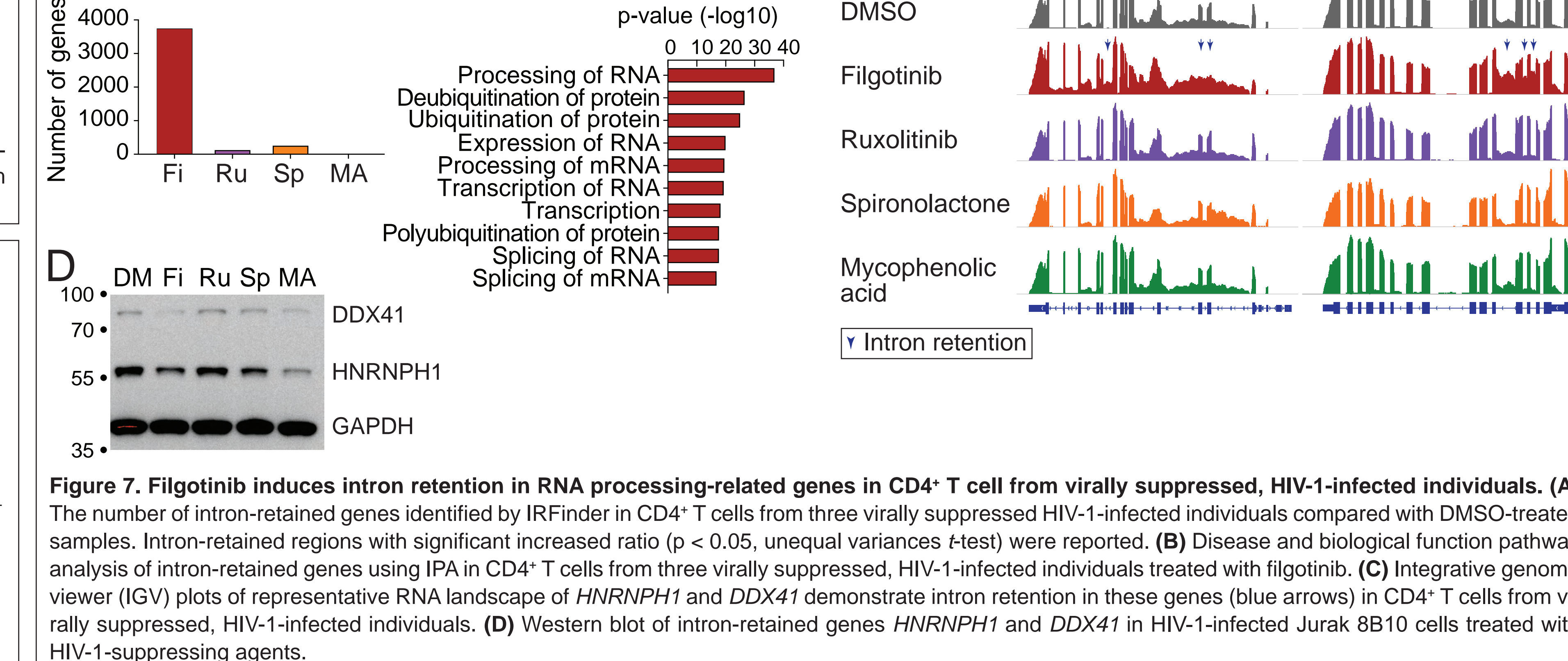


**Figure 7.** Filgotinib induces intron retention in RNA processing-related genes in CD4<sup>+</sup> T cell from virally suppressed, HIV-1-infected individuals. (A) The number of intron-retained genes identified by IRFinder in CD4<sup>+</sup> T cells from three virally suppressed HIV-1-infected individuals compared with DMSO-treated samples. Intron-retained regions with significant increased ratio (p < 0.05, unequal variances t-test) were reported. (B) Disease and biological function pathway analysis of intron-retained genes using IPA in CD4<sup>+</sup> T cells from three virally suppressed, HIV-1-infected individuals treated with filgotinib. (C) Integrative genome viewer (IGV) plots of representative RNA landscape of *HNRNPH1* and *DDX41* demonstrate intron retention in these genes (blue arrows) in CD4<sup>+</sup> T cells from virally suppressed, HIV-1-infected individuals. (D) Western blot of intron-retained genes *HNRNPH1* and *DDX41* in HIV-1-infected Jurkat 8B10 cells treated with HIV-1-suppressing agents.

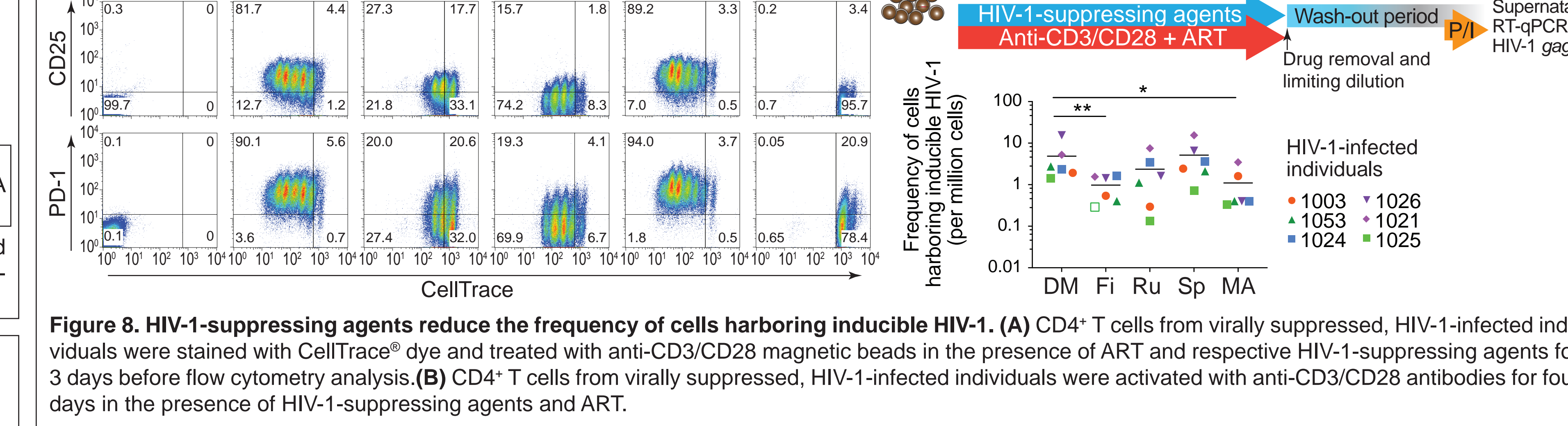


**Figure 8.** HIV-1-suppressing agents reduce the frequency of cells harboring inducible HIV-1. (A) CD4<sup>+</sup> T cells from virally suppressed, HIV-1-infected individuals were stained with CellTrace<sup>®</sup> dye and treated with anti-CD3/CD28 magnetic beads in the presence of ART and respective HIV-1-suppressing agents for 3 days before flow cytometry analysis. (B) CD4<sup>+</sup> T cells from virally suppressed, HIV-1-infected individuals were activated with anti-CD3/CD28 antibodies for four days in the presence of HIV-1-suppressing agents and ART.

## CONCLUSION

Overall, a combination of drug screening and transcriptome analysis identified the landscape of cellular pathways critical for HIV-1 reactivation and a novel HIV-1-suppressing agent filgotinib. Filgotinib suppresses HIV-1 transcription and reducing the proliferation of HIV-1-infected cells by targeting two different pathways, involving inhibition of T cell activation and modulation of HIV-1-splicing. Therapeutic strategies targeting a combination of these pathways with increased selectivity against HIV-1-infected cells provides a new direction to reduce HIV-1-related immune activation and the expansion of the HIV-1-infected cells.

## ACKNOWLEDGEMENT

We thank all study participants. We thank NIH AIDS Reagents Program. This work is supported by Yale Top Scholar, Rudolf J. Anderson Fellowship, American Foundation for AIDS Research (amfAR), NIH R01 AI141009, R61 DA047037, R21AI118402, W. W. Smith AIDS Research Grant, Johns Hopkins Center for AIDS Research Award P30AI094189, Gilead AIDS Research Grant (Y.-C.H.), Gilead HIV Research Scholar Grant, NIH BEAT-HIV Delaney Collaboratory UM1AI126620 and NIH CHEETAH P50 AI150464-13.